The 1st International
Symposium on
Hydraulic Measurement

GROIN ARRANGEMENT IN MEANDERING RIVERS

by
Shoji Fukuoka
Professor of Civil and Environmental Engineering
Faculty of Engineering, Hiroshima University, Hiroshima, JAPAN
Akihide Watanabe
Senior Research Engineer, Public Works Research Institute
Ministry of Construction, Ibaraki, JAPAN
and
Tatsuya Nishimura
Engineer, CTI Engineering Company Limited Tokyo, JAPAN

ABSTRACT

In view of the complementary nature of numerical models and hydraulic model tests, a three-dimensional numerical model was developed to determine the optimum arrangement of groins in meandering rivers. Results of calculations showed very good coincidence with those of the authors' large-scale hydraulic experiments with regard to the three-dimensional flow field and river bed variation, irrespective of whether groins are present or not. This model also enabled us to determine the optimum arrangement of groins in rivers with arbitrary bank alignment.

1. INTRODUCTION

The arrangement of groins is determined mainly through on-site inspection and hydraulic model experiments. Because of the close relationship between groin arrangement and the alignment of levees, a simpler, more rational method for determining their arrangement is being called for.(1) The three-dimensional numerical method,(2) although capable of simulating flow regime and bed variation, presents such problems as having to use a difference mesh in the depth direction, as well as the large volume of calculations required to determine bed position anew each time bed variation occurs.

In spite of these problems, development of the three-dimensional numerical method has made possible considerable accuracy in the simulation of hydraulic phenomena in rivers.

With no adequate analytical method for explaining flow and bed variation in groin installed cases, the proper arrangement of groins for reducing transverse bed slope is often determined through large-scale model experiments, which, though capable of determining groin arrangement in river courses of given alignment, do not lend themselves readily to the determination of this arrangement in different river alignments. Hence, a method for mathematically determining groin arrangement in rivers of arbitrary alignment will be applied to design methods not only for groins but also for many other types of hydraulic structures.

Research by Akigusa and Kikkawa, et al.,(3) is representative of research on groins; there have been no investigations of groin arrangements that are effective in connection with planar profiles of river course discussed herein.

Through systematic experimental research at the Public Works Research Institute of the Ministry of Construction, Japan, (4) (5) the authors have developed a basic approach to design methods for groin arrangement. Through this the authors have (1) developed a method for arranging groins upstream and downstream from a river bend of varying curvature in order to reduce transverse bed slope and utilize the cross-sectional area of the river effectively, and (2) revealed the effectiveness of this method in reducing scouring. However, this work did not result in the synthesis of an analytical model that explains the related mechanism.

Hence, in accordance with the approach outlined above, the authors have developed three-dimensional numerical model to determine proper groin arrangement for reducing bed variation and bank erosion in channels with an arbitrary alignment in which width and bed slope change longitudinally.

Next, we used this model to examine and verify the validity of groin arrangements that reduce cross-sectional scouring depth and the lateral bed slope in order to alleviate bank erosion.

2. THE FLOW CALCULATION IN THE THREE-DIMENSIONAL MODEL

2.1 Basic equation of flow

The coordinate system used is the orthogonal curvilinear coordinate system shown in Fig. 1, in which the downstream direction is defined as the s-axis; the lateral direction, which intersects the s-axis, as the n-axis; and the perpendicular direction as the z-axis. Hydrostatic pressure distribution is assumed in the equation of motion for the z-direction. Substituting the continuity equation (derived by integrating from bottom z_0 to height z) into the equation of motion for the s- and n-direction produces the following equation.

$$u\frac{\partial u}{\partial s}+v\frac{\partial u}{\partial n}-\left(\frac{\partial}{\partial s}\int_{z_0}^{z}u\,dz+\frac{1}{r}\frac{\partial}{\partial n}\int_{z_0}^{z}r\,v\,dz\right)\frac{\partial u}{\partial z}+\frac{uv}{r}=-g\frac{\partial H}{\partial s}+\frac{\partial}{\partial s}\left(\varepsilon\frac{\partial u}{\partial s}\right)+\frac{\partial}{\partial n}\left(\varepsilon\frac{\partial u}{\partial n}\right)+\frac{\partial}{\partial z}\left(\varepsilon\frac{\partial u}{\partial z}\right) \quad \cdots\cdots\cdots\cdots\cdots\cdots (1)$$

$$u\frac{\partial v}{\partial s}+v\frac{\partial v}{\partial n}-\left(\frac{\partial}{\partial s}\int_{z_0}^{z}u\,dz+\frac{1}{r}\frac{\partial}{\partial n}\int_{z_0}^{z}r\,v\,dz\right)\frac{\partial v}{\partial z}-\frac{u^2}{r}=-g\frac{\partial H}{\partial n}+\frac{\partial}{\partial s}\left(\varepsilon\frac{\partial v}{\partial s}\right)+\frac{\partial}{\partial n}\left(\varepsilon\frac{\partial v}{\partial n}\right)+\frac{\partial}{\partial z}\left(\varepsilon\frac{\partial v}{\partial z}\right) \quad \cdots\cdots\cdots\cdots\cdots\cdots (2)$$

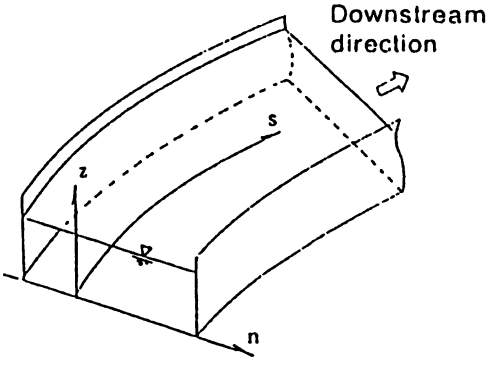

Fig. 1. Definition of the coordinate system

where u and v represent velocity in the s- and n-direction, respectively; H, water level; ρ, water density; r, radius of curvature; g, gravitational acceleration; and ε, coefficient of eddy viscosity, which here is assigned $\varepsilon = \kappa u_* h/6$.
where u_* is the frictional velocity; h, depth; and κ, Karman's constant.
Integrating the continuity equation from the bed to surface and using the kinematic conditions at the surface and bed results in the following.

$$\frac{\partial (u_0 h)}{\partial s}+\frac{1}{r}\frac{\partial (r\,v_0 h)}{\partial n}=0 \quad \cdots\cdots\cdots\cdots (3)$$

where u_0 and v_0 are the depth-averaged velocity for u and v, respectively.
The boundary conditions assigned are discharge (for the upstream end) and water level (downstream end).

2.2 Discretizing the equation of motion according to Galerkin's method and method of calculation

The depth-direction distributions of velocities u and v in the s- and n-directions can be approximated by synthesizing the cosine function. Here, this is expressed by the three terms in the equation below.

$$u(s,n,z)=\sum_{m=0}^{2}u_m(s,n)\cos m\pi z/h$$

$$v(s,n,z)=\sum_{m=0}^{2}v_m(s,n)\cos m\pi z/h \quad \cdots\cdots\cdots (4)$$

When the equation of motion is discretized by substituting equation (4) into equations (1) and (2), multiplying by $\cos l\pi z$ (l=0,1,2) as the weight function, and integrating from the bed to surface, equation (5) and the similar equation are obtained.

$$
\begin{aligned}
&\left(\frac{\partial u_0^2}{\partial s}+\frac{\partial u_0 v_0}{\partial n}+\frac{u_0 v_0}{r}\right)\int_0^1 \cos l\pi z'\,dz' \\
&+\left(2\frac{\partial u_0 u_j}{\partial s}+\frac{\partial u_0 v_j}{\partial n}+\frac{\partial u_j v_0}{\partial n}+\frac{2u_0 v_j}{r}+\frac{2u_j v_0}{r}\right) \\
&\quad\times\int_0^1 \cos i\pi z'\cos l\pi z'\,dz' \\
&+\left(2\frac{\partial u_i u_j}{\partial s}+\frac{\partial u_i v_j}{\partial n}+\frac{2u_i v_j}{r}\right) \\
&\quad\times\int_0^1 \cos i\pi z'\cos j\pi z'\cos l\pi z'\,dz' \\
&+u_0\left(\frac{\partial u_j}{\partial s}+\frac{\partial v_j}{\partial n}+\frac{v_j}{r}\right)\int_0^1 \frac{\sin i\pi z'}{i\pi}\cos l\pi z'\,dz' \\
&+u_i\left(\frac{\partial u_j}{\partial s}+\frac{\partial v_j}{\partial n}+\frac{v_j}{r}\right)\int_0^1 \frac{\sin i\pi z'}{i\pi}\cos j\pi z'\cos l\pi z'\,dz' \\
&=-g\frac{\partial H}{\partial s}\int_0^1 \cos l\pi z'\,dz' \\
&\quad-\frac{\tau_{s0}}{\rho h}-il\pi^2\varepsilon u_i\int_0^1 \sin i\pi z'\sin l\pi z'\,dz' \\
&+\left(\frac{\partial}{\partial s}\left(\varepsilon\frac{\partial u_0}{\partial s}\right)+\frac{\partial}{\partial n}\left(\varepsilon\frac{\partial u_0}{\partial n}\right)\right)\int_0^1 \cos l\pi z'\,dz' \\
&+\left(\frac{\partial}{\partial s}\left(\varepsilon\frac{\partial u_j}{\partial s}\right)+\frac{\partial}{\partial n}\left(\varepsilon\frac{\partial u_j}{\partial n}\right)\right)\int_0^1 \cos i\pi z'\cos l\pi z'\,dz'
\end{aligned}
\qquad \text{---------- (5)}
$$

where $z'=(z-z_0)/h$, i,j is the combination of the cosine functions shown in equation (4); l is the weight (l=0,1,2) according to Galerkin's method; and τ_{s0} and τ_{n0} are the bed shearing force in the s- and n-directions, which are represented with the following equations.

$$
\begin{aligned}
\tau_{s0} &= \rho C_b u_b \sqrt{u_b^2+v_b^2} \\
\tau_{n0} &= \rho C_b v_b \sqrt{u_b^2+v_b^2}
\end{aligned}
\qquad \text{--------- (6)}
$$

where C_b is the bed friction coefficient and u_b and v_b are the respective velocities at the bed. The equations of motion discretized according to Galerkin's method are then used to determine u_0 and v_0 when l=0; u_1 and v_1 when l=1; and u_2 and v_2 when l=2.

We now make finite difference of equations of motion and continuity equation discretized according to Galerkin's method. To perform this difference, the s- and n-directions are respectively designated as j and i, while u and v, H and h are determined with the calculation grid shown in Fig. 2.

The linear equation obtained thus is then used to determine u_0 and v_0. The values when l=1 and l=2 are also determined in the same manner using the linear equations with u_1, u_2, v_1 and v_2.

As continuity equation (3), integrated in the depth direction, has a discharge balance of zero in the shaded area of the graph in Figure 3.

These difference equations produce an equation for water level H, which, when solved, gives the value of water level H (i,j).

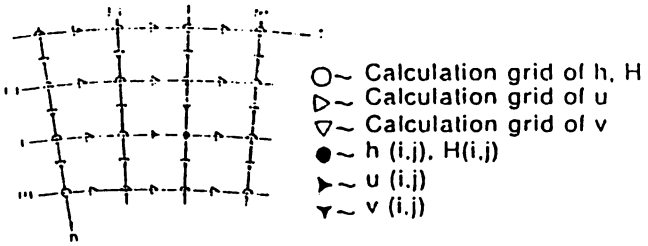

Fig. 2. Grid positions of h, H, u and v

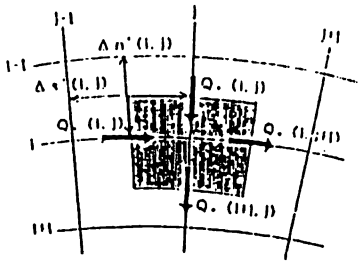

Fig. 3. Differences of the depth-averaged continuity equation

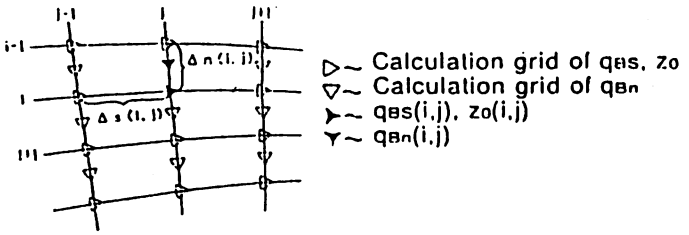

Fig. 4. Grid positions of sediment discharge and bed level

3. CALCULATING BED VARIATION WITH A THREE-DIMENSIONAL MODEL

Changes in bed height are represented with the following equation.

$$\frac{\partial z_o}{\partial t} + \frac{1}{1-\lambda}\left(\frac{\partial q_{bs}}{\partial s} + \frac{1}{r}\frac{\partial r q_{bn}}{\partial n}\right) = 0 \qquad (7)$$

where t is time; z_o, bed height; λ, bed material porosity; and q_{bs} and q_{bn}, bed load transport per unit of width in the s- and n-directions. q_{bs} is calculated with the Meyer-Peter-Muller equation, and q_{bn} is calculated with Hasegawa's equation. (6)

The calculation grid for q_{bs} and q_{bn} and bed height z_o is arranged as shown in Fig. 4.

By alternately solving equations (3) and (5) and equation (7) by difference method repeatedly, the bed height after the passage of time is successively determined.

When submerged, permeable groins exists in a channel, they affect the flow. However, accurately predicting the flow and bed variation around such submerged, permeable structures is not that easy. With the three-dimensional difference method, in which a calculation mesh is arranged in the direction of depth, it is possible, in principle, to perform calculations using meshes for the rear and front surfaces of the groin by applying the kinematic boundary condition that velocity in the normal direction with respect to the groin is zero. However, this method involves such problems as an enormous amount of calculations and the fact that the results are greatly affected by how difference in the depth direction is performed. Hence, we incorporated the effects of the groin placement on the flow by reducing the flow cross-sectional area in the calculation grid, and by arranging the calculation mesh with groin position.

Dead-water regions are formed between the groins when the latter are spaced roughly 2 times apart, a distance said to bring out groin effectiveness. Because, however, the model used here employs integration in the direction of depth, this phenomenon cannot be reproduced faithfully. Consequently, in three-dimensional flow calculations, the top surface of groins are treated as the river bed (in the section containing the groins), and the area below the height of the top surface of groins is considered to be a dead-water region. The velocity at a bed with this height is considered to be slip velocity u_b and v_b. Also, in bed level calculations it is assumed that no scouring occurs on the top surfaces of groins. Where no groins exist, bed variation is assumed to be caused by a sediment discharge commensurate with the tractive force at that point.

4. COMPARISON WITH OBSERVED RESULTS

4.1 Comparison with experimental results for meandering channels

Let us now compare the calculated results for bed variation in the absence of groins with the results of the experimentation (4) (5). The experimental channel (Fig. 5), a model 1/40 the size of

an actual river, is a meandering channel with a compound cross-section; a main channel whose width changes from 2.0 to 3.0 meters in the downstream direction and whose minimum radius of curvature is 5.2m; and an average depth of 0.15m (channel 1). The experimental conditions are shown in Table 1. The experiment was performed with and without groins in place. In order to determine the effects of the main channel's radius of curvature on bed variation, the channel was then converted into a gently meandering one (channel 2) with a minimum radius of curvature of 7.2m. Unless otherwise stated, the term "channel" used hereinafter shall refer to experimental channel 1. For calculation, the channel was longitudinally divided into 27 sections at intervals of roughly 1.0 to 2.5 meters to reflect actual groin arrangement (discussed below). To avoid instability in the calculations; a mesh in which the main channel and flood channel were separately divided into three and nine sections, respectively, was used. Fig. 6 (contour diagrams of the same bed variation) show that the calculated results correspond, with great accuracy, to actual bed form in the main channel, and that calculated results for maximum scouring depth and maximum deposition height nearly match the corresponding experimental results.

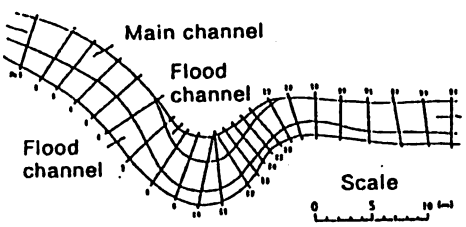

Fig. 5. The experimental channel

Table 1. Experimental conditions 4)5)

Discharge (l/sec.)	150.0
Surface gradient	1/1,000
Average depth (m)	0.15
Width of main channel (m)	2.0 – 3.0
Minimum radius of curvature (m)	5.2, 7.2
Bed material (mm)	0.8
Sediment density	2.65

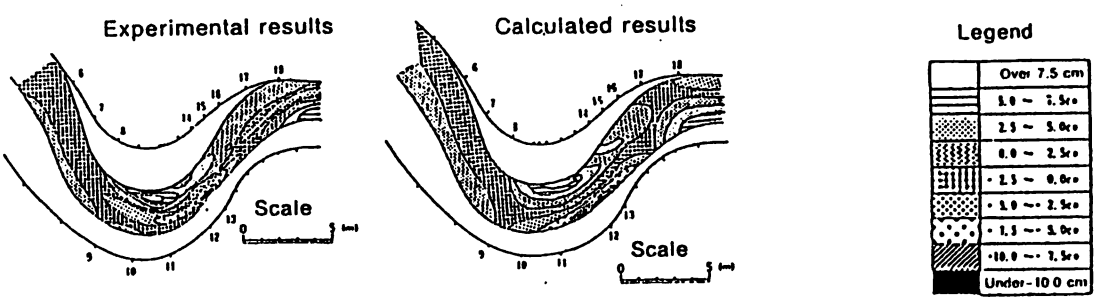

Fig. 6. Bed contour diagrams

4.2 Comparison with experimental results for a channel where groins are present

In their experiment, the authors longitudinally arranged groins in the experimental channel (Fig. 5) to reduce lateral bed slope through an effect on the flow that is equivalent to that achieved through alignment modification. The experiment was performed for five different cases (Fig. 7). The groin arrangement used in Case 3 (i.e., only along the outside bank of the bend) is similar to the groin arrangement commonly used to directly protect the bank requiring fortification. Although this resulted in a shifting of scouring along the outer bank to the front surfaces of the groins, there was almost no reduction in the scouring depth there, and hence not so much change in the degree of flow concentration on the outer bank. There are two plausible ways to ease this flow concentration: (1) giving the channel a more gentle alignment, and (2) arranging groins upstream from the bend along the inner bank to disperse flow concentration and decrease flow curvature so that a calmer flow enters the downstream section where the groins are. First, we shall determine the effects, on outer bank bed scouring and inner bank deposition, of changes in flow curvature caused by upstream groins along the inner bank of the main channel (sections 7 through 9) and downstream groins along the outer bank of the main channel (sections 10 through 15).

Let us compare the calculated results concerning depth-averaged velocity distribution and bed variation mainly with the corresponding results for experimental case 2, which is believed to be the optimum groin arrangement and in which lateral bed slope was lower than in any other case. As shown in Fig. 8, twenty-two submerged, permeable groins (with the specifications and configuration shown in Fig. 9 and Table 2) were arranged along the inner bank of the main channel upstream and along the outer bank of the main channel downstream.

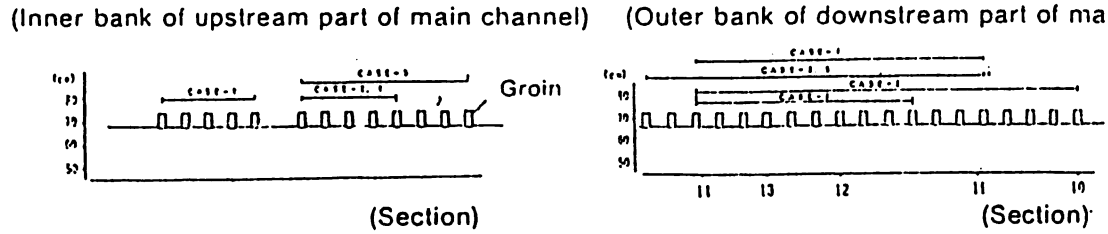

Fig. 7. Groin arrangements

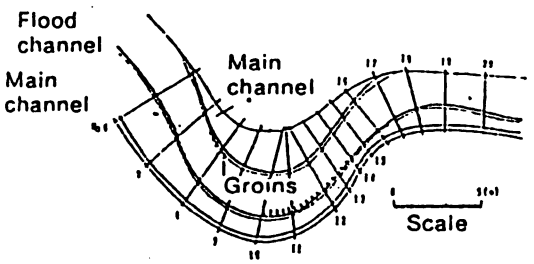

Fig. 8. Groin arrangement (case 2)

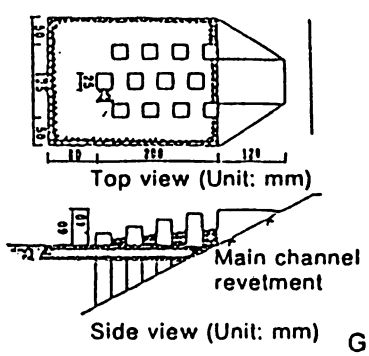

Fig. 9. Groin configuration

Table 2. Groin items (case 2)

Groins along left bank (spaced 40 cm apart)

Number (from upstream end)	1	2	3	4	5
Groin length (cm)	20	20	20	20	20

Groins along right bank (spaced 40 cm apart)

Number (from upstream end)	1	2	3	4	5	6	7	8	9	10	11	12	13	14	15	16	17
Groin length (cm)	20	20	20	20	20	20	20	20	20	20	20	20	20	20	20	20	20

Figs. 10 and 11 are comparisons of calculated and experimental results for, respectively, lateral distribution of depth-averaged velocity u_0 two hours after the flow was begun; and the resultant bed contours. Looking at u_0, we see that the calculated results accurately describe actual flow conditions, i.e., that water velocity is slowed by the groins' deflecting of water along the inner bank of the main channel upstream (section 8) and along the outer bank of the main channel downstream. The bed contour diagrams show that although the calculated results for local bed variation caused by deposition correspond insufficiently to experimental results, the position and size of maximum scouring depth have been accurately predicted. The margin of error in the prediction of maximum scouring depth was roughly 5% in these experimental cases.

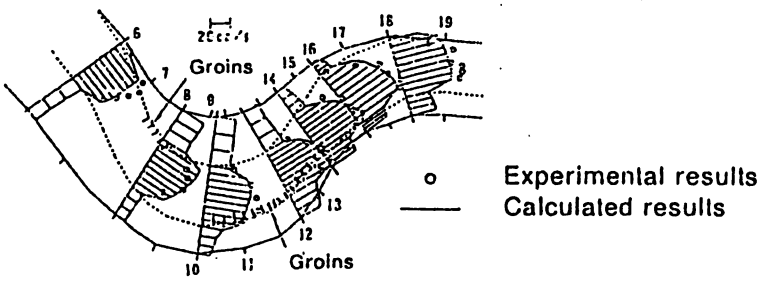

Fig. 10. Lateral distribution of depth-averaged velocity uo when groins are present (case 2)

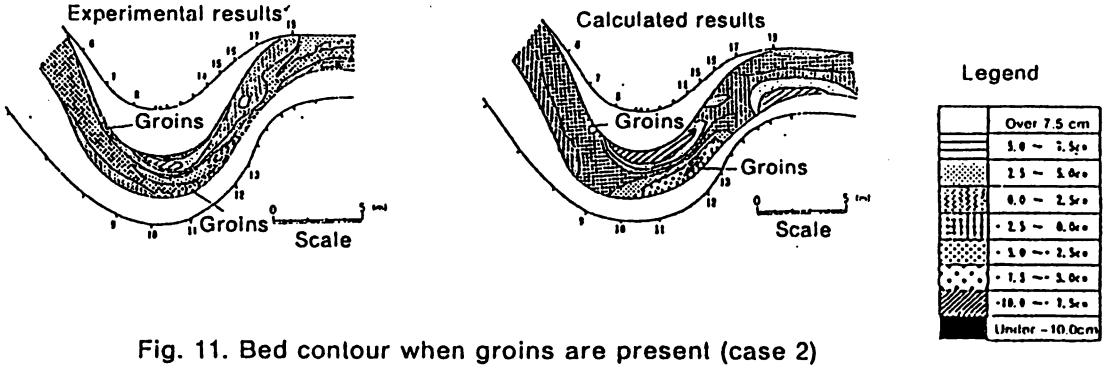

Fig. 11. Bed contour when groins are present (case 2)

5. GROIN ARRANGEMENT

Fig. 12 contains the experimental results and corresponding calculated results for maximum scouring depth when, in bends with small curvature (channel 1) and large curvature (channel 2), groins are arranged upstream and downstream; not arranged anywhere in the channel; and arranged downstream only. It clearly shows that increasing the bend's radius of curvature (from 5.2 to 7.4 meters) results in a smaller scouring depth along the outer bank, and that arranging groins along both the inner and outer banks is much more effective in reducing maximum scouring depth along the outer bank than arranging groins along the outer bank only. We can also see that for this experimental channel, which has two radiuses of curvature, maximum scouring depth in a channel with a central radius of curvature of r_c=5.2 meters and groins arranged upstream and downstream is roughly the same as maximum scouring depth in a channel where, instead of using groins, the main channel's central radius of curvature has been increased to r_c=7.4 meters to increase the flow's radius of curvature. This demonstrates that in rivers where channel alignment cannot be smoothened, the similar results can be achieved by properly arranging groins in this manner. Fig. 12 clearly shows that maximum scouring depth can be reduced with a combination of groins arranged along the inner bank of the main channel upstream and along the outer bank of the main channel downstream.

Next, using experimental and calculated results, we determine which type of upstream and downstream arrangements are effective in reducing scouring. The arrangements of groins along the main channel's inner bank upstream and along the main channel's outer bank downstream were changed as shown in Fig. 8. As can be seen in Fig. 13 (a comparison of the calculated and experimental results, in which the horizontal axis is the position of upstream groins and the vertical axis is maximum deposition height [bottom] and maximum scouring depth [top] for each case, minus their corresponding values when no groins were present), smaller reductions in maximum scouring depth and maximum deposition height mean a smaller lateral bed slope and hence smaller flow concentration, which is the desired outcome. (The symbols o and ▲ represent the central positions of the upstream groin array, while the solid and broken lines represent groin boundaries.)

Looking at this diagram, it can be seen that near section 8 would be the optimum position for upstream groins along the inner bank of the main channel (judging from the fact that deposition

height and scouring depth when groins were positioned near section 7 (in case 1) and downstream from section 8 (in case 5) were almost the same as when no groins were present), and that the optimum position for downstream groins along the outer bank of the main channel was between sections 10 and 14 (as maximum scouring depth was lowest when the groins were arranged here in case 2). Thus, calculated results, though differing slightly with those obtained experimentally, reflect with great accuracy the relationship between this groin arrangement and maximum scouring depth and maximum deposition height.

The above demonstrates that the mathematical model developed through this research can predict flow in a channel with arbitrary alignment and serve as a method for determining the optimum groin arrangement for minimizing lateral bed slope and making maximum use of the cross-sectional area of the channel.

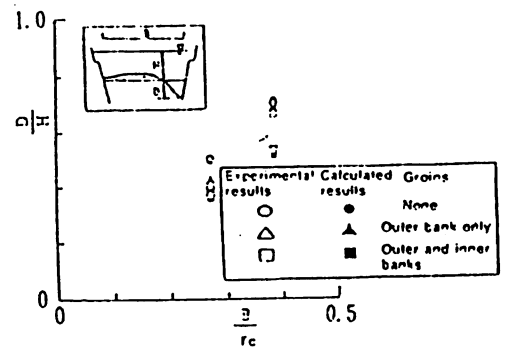

Fig. 12: Relationship between curvature and maximum scouring depth

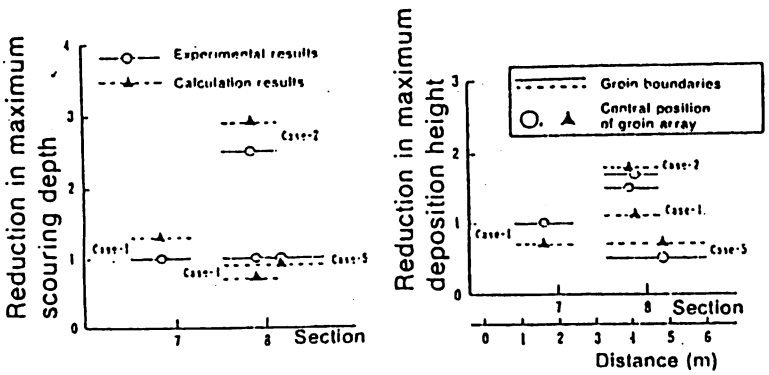

Fig 13. Relationship between groin arrangement and maximum scouring depth and maximum deposition height

6. CONCLUSION

The main conclusions reached are as follows.

(1) Large-scale model experiments have shown that in order to reduce bed scouring along the outer bank of a river bend, groins must be arranged -- longitudinally and in a way that brings out their integrated effectiveness -- not only along the outer bank but also along the opposite bank upstream.

(2) Results of calculations using three-dimensional numerical model also correspond, with great accuracy, to changes in maximum scouring depth and maximum deposition height observed in these large-scale model experiments, in which groins were arranged in different positions along the inner bank upstream and along the outer bank downstream.

The mathematical model can be used to determine proper groin arrangement for creating desirable longitudinal and lateral bed profiles in channels with arbitrary alignment.

REFERENCES

1) Fukuoka, S.: Examples of River Scouring and Its Countermeasures, 2nd Symposium of Rivers and Coasts, JSCE, pp.49 – 70, 1988, (in Japanese)
2) Shimizu, Y., Yamaguchi, H. and Itakura, T.: Three-dimensional Computation of Flow and Bed Deformation, Journal of Hydraulic Engineering, Vol.116, pp.1090 – 1108, 1990.
3) Akigusa, I., Kikkawa, H., Sakagami, Y., Ashida, K. and Tsuchiya, A.: Study on Groin, Report of Public Works Research Institute, No.107, 1960, (in Japanese)
4) Fukuoka, S., Takahashi, A. and Watanabe, A.: Arrangement of Groins and its Erosion Reduction, Bulletin of Public Works Rersearch Institute, No.2640, 1988, (in Japanese)
5) Fukuoka, S., Watanabe, A. and Nishimura, T.: On the Groin Arrangement in Meandering Rivers, Hydraulic and Sanitary Engineering, Proc. JSCE, No.443. 11 – 18, pp.27 – 36, 1992, (in Japanese)
6) Hasegawa, K.:. A Study of Flows and Bed Topographies in Meandering Channels, Proc. JSCE, No.338, pp.105 – 114, 1983, (in Japanese)